Control of Dual-User Haptic Training System With Online Authority Adjustment: An Observer-Based Adaptive Robust Scheme

Mohammad Motaharifar, *Student Member, IEEE*, Hamid D. Taghirad, *Senior Member, IEEE*, Keyvan Hashtrudi-Zaad, *Senior Member, IEEE*, and Seyed Farzad Mohammadi

***Abstract*— The design problem for the control a dual-user haptic surgical training system is studied in this article. The system allows the trainee to perform the task on a virtual environment, while the trainer is able to interfere in the operation and correct probable mistakes made by the trainee. The proposed methodology allows the trainer to transfer the task authority to or from the trainee in real time. The robust adaptive nature of the controller ensures position tracking. The stability of the closed-loop system is analyzed using the input-to-output stability approach and the small-gain theorem. Simulation and experimental results are presented to validate the effectiveness of the proposed control scheme.**

***Index Terms*— Dual-user haptics, robust adaptive control, stability, surgical training, task dominance.**

I. Introduction

HAPTIC systems provide a more tangible perception of reality for users interacting with virtual environments. Due to this feature, haptic technology has received a great deal of interest in applications such as medical simulations, computer-aided design, and gaming [1], [2]. A more recent advancement in kinesthetic haptics is in multiuser haptic systems, particularly dual-user systems, which have applications in surgical training [3] and robotic telerehabilitation [4], [5]. In the former, which is the focus of this article, the trainer and the trainee interactively perform surgical tasks on a shared virtual environment. Such technology provides a suitable training framework within which the trainee can learn the surgical skills using the corrective haptic cues from the trainer.

The ultimate objective of the control design for dual-user haptic systems is to provide robust stability of the closed-loop system against uncertainties with sufficient performance. To this purpose, several control architectures have been proposed for dual-user haptic systems. In [6], an H_∞-based shared control scheme for a dual-user haptic system was proposed. By introducing the concept of dominance factor, the authority of each user over the task was determined. Utilizing the concept of dominance factor, a six-channel shared control architecture was developed for dual-user haptic system [7]. These control architectures do not consider dynamic nonlinearities of the robots, which is a significant issue in this field. To address the dynamic nonlinearities of the robots, a few control architectures have been proposed, such as the $PD+d$ structure [8]. However, the most important shortcoming of these works is their inability to transfer task authority between the trainer and the trainee in real time [6]–[8]. Having said that mechanisms should be in place to transfer the task authority to the trainer when unanticipated mistakes are made by the trainee, as they may lead to undesirable complications for the patients.

In order to mitigate the above shortcoming, other control methodologies have been proposed with online authority adjustment. For instance, a fuzzy logic-based relative skills assessment approach is proposed in [9] for a dual-user surgery training system. In the proposed expertise-oriented methodology, the trainee's proficiency level is specified relative to the trainer in real time, and the task dominance is adjusted through the assessed proficiency level and fuzzy logic rules. Other methodologies have also considered real-time authority adjustment based on online supervision of the position error [10]. In these investigations, the normalized position error between the trainer and the trainee is utilized to adjust task dominance in real time. However, some limitations can be considered regarding those methodologies [9], [10]. The first limitation of those approaches is the necessity of involving the trainer in every stage of surgical procedures, especially the trivial ones. In other words, it is not possible to grant the trainee the authority to perform subtasks unless the trainer performs the entire details precisely. This is hardly

Manuscript received August 7, 2019; accepted September 30, 2019. Manuscript received in final form October 9, 2019. This work was supported in part by the National Institute for Medical Research Development (NIMAD) under Grant 942314, in part by the Tehran University of Medical Sciences, Tehran, Iran, under Grant 35949-43-01-97, and in part by the K. N. Toosi University of Technology, Tehran, Iran Research Grant. Recommended by Associate Editor G. Hu. *(Corresponding author: Hamid D. Taghirad.)*

M. Motaharifar is with the Advanced Robotics and Automated Systems (ARAS), Industrial Control Center of Excellence, Faculty of Electrical Engineering, K. N. Toosi University of Technology, Tehran 1969764499, Iran, and also with the BioRobotics Research Laboratory, Department of Electrical and Computer Engineering, Queen's University, Kingston, ON K7L 3N6, Canada (e-mail: motaharifar@email.kntu.ac.ir).

H. D. Taghirad is with the Advanced Robotics and Automated Systems (ARAS), Industrial Control Center of Excellence, Faculty of Electrical Engineering, K. N. Toosi University of Technology, Tehran 1969764499, Iran (e-mail: taghirad@kntu.ac.ir).

K. Hashtrudi-Zaad is with the BioRobotics Research Laboratory, Department of Electrical and Computer Engineering, Queen's University, Kingston, ON K7L 3N6, Canada (e-mail: khz@queensu.ca).

S. F. Mohammadi is with the Translational Ophthalmology Research Center, Farabi Eye Hospital, Tehran University of Medical Sciences, Tehran 1336616351, Iran (e-mail: sfmohammadi@tums.ac.ir).

Color versions of one or more of the figures in this article are available online at http://ieeexplore.ieee.org.

Digital Object Identifier 10.1109/TCST.2019.2946943

compatible with the supervisory role of the trainer in which the trainer interferes with the procedure only when it is necessary. Moreover, they have not reported any stability analysis by considering the nonlinearity in the robotic manipulators. The aim of this article is to address these issues by proposing a real-time authority adjustment control architecture for the dual-user surgery training haptic system with an emphasis on the supervisory role of the trainer and analyzing the nonlinear stability of the closed-loop system.

The contribution of this work is to present a new control architecture for the dual-user haptic surgical training with time-varying authority adjustment. The proposed approach is based on allowing the trainee to conduct the surgical operations and be corrected as needed. To this effect, two basic operation modes of the controller are identified as the trainee and trainer dominant modes. These two modes are realized through a proposed control scheme with a soft transition to ensure the smooth response of the system. In the trainee-dominant mode, the trainer needs to know the position of the surgical tool to detect the probable incorrect motion commands made by the trainee. On the other hand, in the trainer-dominant mode, the desired position of the surgical tool should be the position of trainer's haptic console to ensure the full dominance of the trainer over the task. A novel robust adaptive controller, which takes into account the dynamic uncertainties of the robots, is proposed to ensure position tracking in both modes. Furthermore, the surgeons' hand force signals are obtained using a high-gain observer approach. High-gain observers are widely used in the estimation of unknown states [11], [12] and unknown inputs [13] of nonlinear systems. The stability of the closed-loop system is studied using input-to-state stability (ISS) analysis by considering the nonlinear dynamics of the haptic devices.

The rest of this article is organized as follows. The dual-user haptic surgical training system is detailed in Section II. The dynamics of the haptic devices are described in Section III. Section IV elaborates the proposed control structure, while Section V presents its stability analysis. Simulation and experimental results are given in Section VI, and the conclusions are stated in Section VII.

II. System Description

The dual-user haptic surgical training system allows a trainee to conduct the surgical operations on a real or virtual environment and be corrected as needed through the haptic guidance signals from the trainer. The surgical operation is conducted by the trainee, and the trainer is able to interfere with the procedure to correct the trainee's mistakes. As a result, the contact force of the virtual environment is a function of the trainee's hand position and velocity. In our proposed control architecture, the following modes of operation are realized.

1) *Trainee-Dominant Mode:* In this mode, the trainer trusts the trainee's movements. As a result, the trainee is allowed to have full dominance over the tasks. This means that the trainee directly performs the surgical operation with little intervention from the haptic system. On the other hand, the trainer needs to know the position of the surgical tool to figure out the probable wrong motion commands applied by the trainee. As a result, a position tracking control scheme is required at the trainer side.
2) *Trainer-Dominant Mode:* In this mode, the trainer does not approve the trainee's motion commands, and thus, the task authority is transformed to the trainer. In order for the trainer to have full authority over the surgical operation, the position of the surgical tool, which is connected to the trainee haptic console should follow the position of trainer haptic console. In addition to the position tracking controller, an additional control term for dealing with the conflicting trainee movements is introduced.

In this article, a control architecture with desired trajectory switching is developed to realize the above modes. In order to ensure smooth transition between the two modes, a soft-switching operation is also introduced. The proposed control architecture will be presented after providing preliminary information on the system dynamics.

III. System Dynamics

The dynamics of a dual-user haptic system consisting of two n-DOF robot manipulators can be expressed as [14]

$$M_i(q_i)\ddot{q}_i + C_i(q_i,\dot{q}_i)\dot{q}_i + G_i(q_i) = u_i + J_i^T(q_i) f_{hi} \quad (1)$$

where $q_i \in \mathbb{R}^{n\times 1}$ are the joint displacement vectors, $M_i(q_i) \in \mathbb{R}^{n\times n}$ are the inertia matrices, $C_i(q_i,\dot{q}_i) \in \mathbb{R}^{n\times n}$ are the centripetal and Coriolis matrices, $G_i(q_i) \in \mathbb{R}^{n\times 1}$ are gravity vectors, $u_i \in \mathbb{R}^{n\times 1}$ denote the control torque vectors, $f_{hi} \in \mathbb{R}^{n\times 1}$ are the forces applied by the surgeons, and $J_i(q_i)$ represent the Jacobian matrix of the haptic devices. Throughout this article, the subscript i denotes the haptic console #1 for $i = 1$ and haptic console # 2 for $i = 2$.

Let us review some useful properties of the dynamic equations (1) as follows [14].

Property 1. The inertia matrix $M_i(q_i)$ is symmetric. In addition, it is shown that $\lambda_{mi} I_{n\times n} \le M_i(q_i) \le \lambda_{Mi} I_{n\times n}$ where λ_{mi} and λ_{Mi} are positive real numbers.

Property 2. The matrix $\dot{M}_i(q_i) - 2C_i(q_i,\dot{q}_i)$ is skew symmetric, which means that $x^T\big(\dot{M}_i(q_i) - 2C_i(q_i,\dot{q}_i)\big)x = 0$ $\forall x \in \mathbb{R}^n$

Property 3. The left-hand side of the model (1) may be expressed as $M_i(q_i)\ddot{q}_i + C_i(q_i,\dot{q}_i)\dot{q}_i + G_i(q_i) = Y_i(q_i,\dot{q}_i,\dot{q}_i,\ddot{q}_i)\theta_i$ where, Y_i is called the regressor and θ_i is the vector of dynamic parameters. This parameterization can also be extended as

$$M_i(q_i)a_i + C_i(q_i,\dot{q}_i)v_i + G_i(q_i) = Y_i(q_i,\dot{q}_i,v_i,a_i)\theta_i. \quad (2)$$

The following two assumptions are considered for the forces applied by the environment and the operators.

Assumption 1: The environment force denoted by f_e is defined as $f_e = f(q_2,\dot{q}_2)$ and satisfies the Lipschitz condition for both its variables [15], that is, $f_e \le L_e(\|q_2\| + \|\dot{q}_2\|)$.

Assumption 2: The operators hand forces are modeled by the linear time-invariant mass-damper-spring system [16], [17]

$$f_{hi} = f_{hi}^* - M_{hi}\ddot{x}_i - B_{hi}\dot{x}_i - K_{hi}x_i \quad (3)$$

This article has been accepted for inclusion in a future issue of this journal. Content is final as presented, with the exception of pagination.

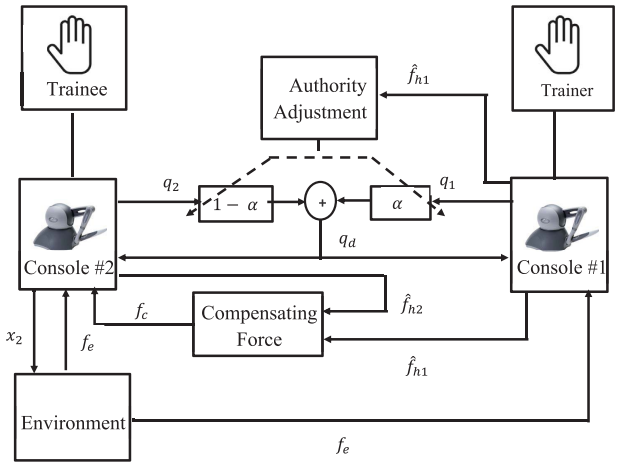

Fig. 1. Proposed dual-user haptic training system.

where f_{hi}^* is the exogenous force generated by the operator #i, and M_{hi}, B_{hi}, and K_{hi} are the positive definite matrices corresponding to mass, damping, and stiffness of the operator #i, respectively.

IV. Proposed Control Architecture

The block diagram of the proposed control architecture is depicted in Fig. 1. In the proposed scheme, the authority of each surgeon over the task is determined by the dominance factor α where $0 \leq \alpha \leq 1$. In the steady state, the value of the dominance factor might be either 0 or 1, and the values between 0 and 1 are included to ensure soft transition between the two modes. The case $\alpha = 0$ corresponds to the trainee-dominant mode, whereas the case $\alpha = 1$ represents the trainer-dominant mode. The trainer has the privilege to transform task dominance between herself/himself and the trainee in real-time. The dominance factor is determined by the magnitude of the force exerted by the trainer. In order to smooth out short term fluctuations and underline longer term trends, the moving average of the force with a fixed window size denoted by w is proposed to determine the magnitude of force as

$$\bar{f}_{h1} = \frac{1}{w}\int_{t-w}^{t} \|f_{h1}\| dt. \tag{4}$$

If the magnitude of the force applied by the trainer is less than a predefined value, the dominance factor is set to zero and the surgical operation is performed solely by the trainee. Intuitively, the low magnitude of the applied force indicates that the trainer holds the haptic console at ease. In the event that the force exerted by the trainer is greater than the predefined value, the dominance factor is set to unity, and the task authority is transferred to the trainer. Note that, large exerted force intuitively implies that the trainer tightly grasps the surgical tool. In order to provide soft switching between the two mentioned modes, a sinusoidal function is utilized as the transition state. As a result, the dominance factor is mathematically formulated as

$$\alpha = \begin{cases} 0, & \bar{f}_{h1} \leq \beta_1 \\ \sin\dfrac{\pi(\bar{f}_{h1}-\beta_1)}{2(\Delta\beta)}, & \beta_1 \leq \bar{f}_{h1} \leq \beta_2 \\ 1, & \bar{f}_{h1} \geq \beta_2 \end{cases} \tag{5}$$

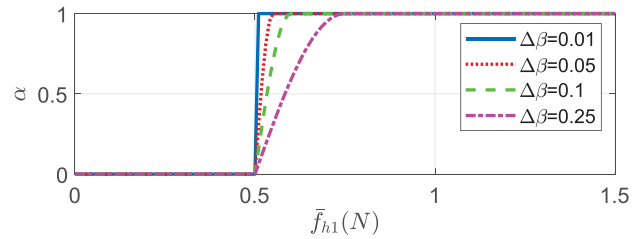

Fig. 2. Transition state of dominance factor for various $\Delta\beta$ with $\beta_1 = 0.5$.

where β_1 and β_2 are some threshold values and $\Delta\beta := \beta_2 - \beta_1$. The above expression shows that if the magnitude of the force exerted by the trainer is less than β_1, the dominance factor is zero, and for the magnitude of force greater than β_2, the dominance factor is unity, while a sinusoid transition function is considered between the two thresholds. The transition state is considered to avoid abrupt switching of the control scheme and to ensure the smooth behavior of the controller. The duration of the transition state is simply set by the parameter $\Delta\beta$. The transition state of the dominance factor is compared for different values of $\Delta\beta$ in Fig. 2. It should be note that the duration of transition should be considered sufficiently small to ensure a prompt action by the controller. Other suitable smooth functions, such as sigmoid, can also be considered to adjust the sharpness of the transition phase.

After determining the dominance factor, the desired positions of the haptic consoles are defined as

$$q_{d1} = q_{d2} = \alpha q_1 + (1-\alpha) q_2. \tag{6}$$

Under the above relationship, in the trainee-dominant mode where $\alpha = 0$, the position of the trainee is the desired position of both haptic consoles. First, on the grounds that the trainer's haptic console tracks the position of the trainee, the trainer receives the position information of the surgical tool. In addition, the desired position of the trainee haptic console is the position of the trainee haptic console itself. This means that the position error of the trainee haptic console is zero, and the trainee is able to freely conduct the surgical operation without any interference from the haptic system.

On the other hand, in the trainer-dominant mode where $\alpha = 1$, the position of the trainer is the desired position of both haptic consoles. As already explained, the trainer-dominant mode occurs in the event that the trainer intends to fully transfer the task authority to himself/herself. In this mode, the trainee haptic consoles, and consequently, the surgical tool tracks the position of the trainer haptic console. Furthermore, since the position error of the trainer haptic console is zero, the trainer freely performs the surgery without any unfavorable interference.

To realize the above scheme, the following control law is developed for the haptic consoles # 1 and # 2:

$$\begin{aligned} u_i = {} & \hat{M}_i(q_i)\Lambda_i(\dot{q}_{di} - \dot{q}_i) + \hat{C}_i(q_i, \dot{q}_i)\Lambda_i(q_{di} - q_i) \\ & + \hat{G}_i(q_i) - K_i(\dot{q}_i + \Lambda_i(q_i - q_{di})) + J_i^T(q_i) f_{ri} \end{aligned} \tag{7}$$

where $\Lambda_i \in \mathbb{R}^{n\times n}$ and $K_i \in \mathbb{R}^{n\times n}$ are positive definite matrices, and the notation $\hat{(\cdot)}$ denotes the computed value of $(\cdot)$ that will be detailed later. Furthermore, f_{ri} is a force reflecting

term that will be explained later. It can be concluded from Property 3 that the control law (7) is equivalent to

$$u_i = Y_i\hat{\theta}_i - K_i(\dot{q}_i + \Lambda_i(q_i - q_{di})) + J_i^T(q_i)f_{ri} \tag{8}$$

where $Y_i = Y_i(q_i, \dot{q}_i, \Lambda_i(q_i - q_{di}), \Lambda_i(\dot{q}_{di} - \dot{q}_i))$. Now, define

$$r_i = \dot{q}_i + \Lambda_i\tilde{q}_i \tag{9}$$

where $\tilde{q}_i = q_i - q_{di}$. The control law (8) is combined with the dynamic (1) to form the closed-loop dynamic equation

$$\begin{aligned} M_i(q_i)\dot{r}_i + C_i(q_i, \dot{q}_i)r_i + K_i r_i \\ = Y_i(\hat{\theta}_i - \theta_i)l + J_i^T(q_i)(f_{hi} + f_{ri}). \end{aligned} \tag{10}$$

The estimate variable $\hat{\theta}_i$ in (8) is selected as

$$\hat{\theta}_i = \theta_i^* + \delta\theta_i. \tag{11}$$

Here, θ_i^* is the nominal value of θ_i and satisfies the inequality

$$\|\theta_i - \theta_i^*\| \leq \xi_i \tag{12}$$

where the uncertainty bound ξ_i is presumed to be unknown. The supplementary control term $\delta\theta_i$ is defined as $\delta\theta_i = -\hat{\xi}_i \mathrm{sgn}(Y_2^T r_2)$. Notably, continuous approximations of the sgn(.) function such as sat(.) function may be used in the real implementations to make the response more smooth. In addition, the estimated uncertainty bound $\hat{\xi}_i$ is obtained from the following adaptation law

$$\dot{\hat{\xi}}_i = \gamma_i \left\| r_i^T Y_i \right\|_1 - \sigma_i\left(\hat{\xi}_i - \xi_i^*\right) \tag{13}$$

where γ_i is the adaptation gain, $\|.\|_1$ represents the l_1-norm, σ is an arbitrary positive constant, and ξ_i^* is the nominal value of ξ_i. Therefore, the following error dynamics is concluded from (13):

$$\dot{\tilde{\xi}}_i = -\gamma_i \left\| r_i^T Y_i \right\|_1 - \sigma_i\left(\tilde{\xi}_i - \tilde{\xi}_i^*\right) \tag{14}$$

where $\tilde{\xi}_i^* = \xi_i - \xi_i^*$.

Next, the force reflection term is defined for each haptic console. For the haptic console #1, the role of the force reflection control term is to recreate the sense of touch with the environment for the trainer. Thus, the force reflection term for the haptic console #1 is defined as

$$f_{r1} = f_e. \tag{15}$$

On the other hand, the force reflection term of the haptic console #2 has two objectives, namely, to provide the environment contact force, and to reduce conflicts between the trainer and the trainee. The first objective is satisfied similar to the haptic console #1 by simply including the environment contact force in the force reflection signal. In order to satisfy the second objective, the following norm of the difference between the observed trainer's and trainee's forces, that is,

$$\rho = \|\hat{f}_{h1} - \hat{f}_{h2}\| \tag{16}$$

is utilized to determine if and to what extent the commands applied by the two surgeons are in conflict. Then, based on the computed metric, it is decided whether or not a compensating term is required to reduce the conflict. Therefore, f_{r2} is defined as

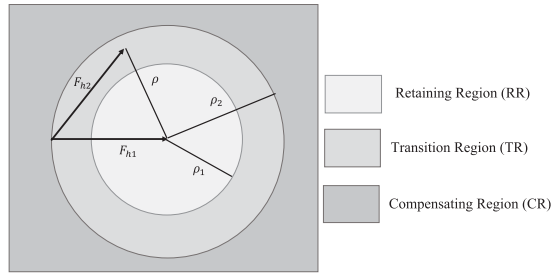

Fig. 3. Regions determining the compensating force reflection.

$$f_{r2} = f_e + f_c \tag{17}$$

where f_c is the compensating force reflection term and it compensates the conflicts between the two users through partial blockage of the trainee's hand force. Fig. 3 illustrates the strategy adopted to resolve the conflict, which is based on using the value of ρ, to define the following three regions.

1) *Retaining Region (RR)*: In this region, the distance between the force vectors applied by the operators is less than the constant value ρ_1, meaning that the vectors f_{h1} and f_{h2} are sufficiently close. The force applied by the trainee does not cause any considerable adverse effect since it is almost at the same magnitude and direction with the force applied by the trainer. As a result, no compensation term is required in this region, and the value of f_c is zero.
2) *Compensating Region (CR)*: In this region, the distance between f_{h1} and f_{h2} is too large to exceed a constant value ρ_2. Due to the great difference between the forces applied by the operators, it is possible that the trainee might induce some unfavorable influence on the position of the surgical tool. Therefore, it is necessary to reduce the conflict between the trainer and the trainee by applying the compensating force reflection term.
3) *Transition Region (TR)*: This region is included to have a smooth transition between the previously mentioned regions. A linear transition function is proposed to ensure soft switching and avoid sudden change between a zero and nonzero force reflection term.

The compensating force f_c is considered to be directly proportional to α; thus, it is nonzero only when $\alpha \neq 0$. In other words, no compensating force is applied to the trainee in the trainee-dominant mode and full compensation is provided in the trainer-dominant mode. Based on the above discussions, the compensating force reflection term is defined as

$$f_c = \alpha\psi(\hat{f}_{h2}) \tag{18}$$

where $\psi(\gamma) = [\psi_1(\gamma_1), \psi_2(\gamma_2), \ldots, \psi_n(\gamma_n)]^T$ and the function $\psi_i(\gamma_i)$ is defined as

$$\psi_i(\gamma_i) = \begin{cases} 0, & \rho \leq \rho_1, \text{ i.e. RR} \\ \left(\dfrac{\rho - \rho_1}{\rho_1 - \rho_2}\right)\mathrm{sat}(\gamma_i), & \rho_1 \leq \rho \leq \rho_2, \text{ i.e. TR} \\ -\mathrm{sat}(\gamma_i), & \rho \geq \rho_2, \text{ i.e. CR.} \end{cases} \tag{19}$$

Note that the saturation function is included here to avoid any damage to the actuators.

The next issue is to find the estimation of hand force signals denoted by $\hat{f}_{hi}$. The state variable vector for the dynamic equation of the haptic consoles is defined as $x_i = [x_{i1}^T \quad x_{i2}^T]^T = [q_i^T \quad \dot{q}_i^T]^T$. Thereafter, the state-space representation of the dynamic system (1) is described as

$$\begin{aligned}\dot{x}_{i1} &= x_{i2}\\ \dot{x}_{i2} &= M_i^{-1}(x_{i1})\big(-C_i(x_{i1},x_{i2})x_{i2} - G_i(x_{i1}) + u_i + f_{hi}\big).\end{aligned}$$

Then, the following high-gain observer is utilized to estimate the hand force signals [12]:

$$\begin{aligned}\dot{\hat{x}}_{i1} &= \hat{x}_{i2} + \frac{a_1}{\epsilon}(x_{i1} - \hat{x}_{i1})\\ \dot{\hat{x}}_{i2} &= M_i^{*-1}(\hat{x}_{i1})\big(-C_i^*(\hat{x}_{i1},\hat{x}_{i2})\hat{x}_{i2} - G_i^*(\hat{x}_{i1})\\ &\qquad + u_i\big) + \frac{a_i}{\epsilon^2}(x_{i1} - \hat{x}_{i1})\\ \hat{f}_{hi} &= \frac{a_2}{\epsilon^2}M_i^*(\hat{x}_i)(x_{i1} - \hat{x}_{i1})\end{aligned} \tag{20}$$

where $(\cdot)^*$ denotes the nominal value of $(\cdot)$. The parameter, ϵ, is a sufficiently small positive constant, and the positive values a_1 and a_2 are chosen such that the roots of $\lambda^2 + a_1\lambda + a_2 = 0$ are both in the left-half-plane.

Defining the estimation error $e_i = [e_{i1}^T, e_{i2}^T]^T$ where $e_{ij} = x_{ij} - \hat{x}_{ij}$ for $j = 1, 2$, the dynamic equation of the estimation error is derived as

$$\dot{e}_i = Ae_i + B\Delta_i - HCe_i \tag{21}$$

where

$$A = \begin{bmatrix}0 & 1\\ 0 & 0\end{bmatrix}, B = \begin{bmatrix}0\\ 1\end{bmatrix}, C = \begin{bmatrix}1 & 0\end{bmatrix}, H = \begin{bmatrix}\frac{a_1}{\epsilon}\\ \frac{a_2}{\epsilon^2}\end{bmatrix}$$

and the dynamic uncertainty term Δ_i is defined as

$$\begin{aligned}\Delta_i := {} & M_i^{-1}(x_{i1})(-C_i(x_{i1},x_{i2})x_2 - G_i(x_{i1}))\\ & -\hat{M}_i^{-1}(\hat{x}_{i1})(-\hat{C}_i(\hat{x}_{i1},\hat{x}_{i2})\hat{x}_{i2} - \hat{G}_{i1}(\hat{x}_{i1})).\end{aligned} \tag{22}$$

Then, inspired in [12], we define

$$\zeta_i = \begin{bmatrix}1 & 0\\ 0 & \epsilon\end{bmatrix} e_i. \tag{23}$$

Equation (21) can be rewritten as

$$\epsilon\dot{\zeta}_i = A_0\zeta_i + \epsilon^2 B\Delta_i \tag{24}$$

where

$$A_0 := \begin{bmatrix}-a_1 & 1\\ -a_2 & 0\end{bmatrix}. \tag{25}$$

Since the eigenvalues of A_0 are the roots of $\lambda^2 + a_1\lambda + a_2 = 0$, the matrix A_0 is Hurwitz.

V. Stability Analysis

Our approach for the stability analysis is to first derive a unique formulation for both haptic consoles in the absence of force reflection term and investigate their stability by that formulation in several steps. Afterward, the force reflecting term is included in the stability analysis of each haptic console, followed by the stability of the entire system. At the beginning of this section, the definition of ISS is presented.

Definition 1 [18]: Consider that $f(t,x,u) : [0,\infty) \times \mathbb{R}^n \times \mathbb{R}^m \to \mathbb{R}^n$ is a piecewise continuous function in t and locally Lipschitz in x and u. Then, the nonlinear system $\dot{x} = f(t,x,u)$ is ISS if there exists a class $\mathcal{KL}$ function β and a class $\mathcal{K}$ function γ such that for any initial state x_0 and any bounded input, the inequality $\|x(t)\| \le \beta(\|x_0\|, t) + \gamma(\sup\|u_T(t)\|)$ is satisfied for $0 \le t \le T$.

Lemma 1 establishes a connection between the concept of ISS presented in Definition 1 and the Lyapunov theory.

Lemma 1 [19] : In the sense of Definition 1, the described system is ISS , provided that there exists a continuously differentiable function V such that $\alpha_1(\|x\|) \le V(x) \le \alpha_2(\|x\|)$ and $\dot{V}(x) \le -\alpha_3(\|x\|) + \alpha_4(\|u\|)$ where $\dot{V}$ is the derivative of V along the trajectory solutions of the system, α_1 and α_2 are class $\mathcal{K}_\infty$ functions, and α_3 and α_4 are class $\mathcal{K}$ functions.

The next proposition analyzes the stability of the haptic systems in the absence of force reflection term without considering the dynamics of the operators and the high-gain observer.

Proposition 1: The closed-loop system for the haptic console #i, i.e., (1) and (7), is ISS with respect to the state $[\tilde{q}_i^T, \dot{q}_i, \tilde{\xi}_i^T]^T$ and the input $[\dot{q}_{id}^T, f_{hi}^T, \tilde{\xi}_i^{*T}]^T$, provided that the force reflection term is considered to be zero, i.e., $f_{ri} = 0$.

Proof: Given in the Appendix.

Next, the stability of the haptic devices by considering the dynamics of the operators is investigated. To that effect, it is supposed that the control input u_i of the haptic system (1) is designed such that the ISS Lyapunov function

$$V_i = V_{ik} + V_{ic} \tag{26}$$

makes the system ISS with input including f_{hi}, where V_{ik} is the kinetic energy of the haptic console #i and is given by

$$V_{ik} = \frac{1}{2}\dot{q}_i M_i(q_i)\dot{q}_i. \tag{27}$$

In addition, the functional V_{ic} is determined by the controller. The following proposition uses such assumption and the dynamics of the operators as given in (3) to investigate the ISS stability of the haptic systems with the input including f_{hi}^*

Proposition 2: Suppose that the control input u_i of the haptic system (1) is designed such that the system is ISS with input $\mu = [\eta^T, f_{hi}^T]^T$ and state χ. Then, by considering the dynamics of the operators (3), the system (1) is ISS with input $\mu_a = [\eta^T, f_{hi}^{*T}]^T$ and the state χ.

Proof: Given in the Appendix.

Then, the next proposition investigates the stability of the haptic devices by considering the effect of the high-gain observer.

Proposition 3: Consider again the case that $f_{ri} = 0$. Then, the closed-loop system for the haptic console #i subsystems (1) and (7) together with the high-gain observer (20) is ISS with respect to the state $[\tilde{q}_i^T, \dot{q}_i, \tilde{\xi}_i^T, \zeta_i^T]^T$ and the input $[\dot{q}_{id}^T, f_{hi}^T, \tilde{\xi}_i^*]^T$

Proof: The following Lyapunov function candidate is considered:

$$V_{i2} = V_{i1} + \zeta^T P \zeta \tag{28}$$

where P is the solution of the Lyapunov equation $A_0^T P + P A_0 = -Q$, and Q is a positive definite matrix. Next, the derivative of V_{i2} is calculated as

$$\dot{V}_{i2} = \dot{V}_{i1} - \epsilon^{-1}\zeta^T Q \zeta + 2\epsilon \zeta^T P B \Delta. \tag{29}$$

On the other hand, due to the Lipschitz condition of the dynamic elements of the robot and using Property 1, it is easy to show that there exists positive scalars L_{i1}, L_{i2}, and L_{i3} such that

$$\Delta \leq L_{i1}\|q_i\| + L_{i2}\|\dot{q}_i\| + L_{i3}\|\zeta\|. \tag{30}$$

Then, using Young's inequality [20], it can be verified that

$$\begin{aligned}\dot{V}_{i2} \leq & -d_{i1}\|\tilde{q}_i\|^2 - d_{i2}\|\dot{q}_i\|^2 - d_{i3}|\tilde{\xi}_i|^2 - d_{i4}|\zeta_i|^2 \\ & + d_{i5}\|q_{id}\|^2 + d_{i6}\|\dot{q}_{id}\|^2 + d_{i7}\|f_{hi}\|^2 + d_{i8}\left\|\tilde{\xi}_i^*\right\|^2\end{aligned} \tag{31}$$

where

$$\begin{aligned}d_{i1} &= \frac{3}{4}\lambda_{\min}(\Lambda_i K_i \Lambda_i) \\ d_{i2} &= \frac{3}{4}\lambda_{\min}(K_i) \\ d_{i3} &= \frac{3}{4}\sigma \\ d_{i4} &= \frac{3}{4}\epsilon^{-1}\lambda_{\min}(Q) - \frac{12\epsilon^2 L_{i1}^2 \lambda_{\max}(P)}{\lambda_{\min}(\Lambda_i K_i \Lambda_i)} - \frac{8\epsilon^2 L_{i2}^2 \lambda_{\max}(P)}{\lambda_{\min}(K_i)} \\ d_{i5} &= \frac{4\epsilon^3 L_{i1}^2 \lambda_{\max}(P)}{\lambda_{\min}(Q)} \\ d_{i6} &= \frac{8\lambda_{\max}(\Lambda_i K_i)}{\lambda_{\min}(\Lambda_i K_i \Lambda_i)} \\ d_{i7} &= \frac{1}{\lambda_{\min}(K_i)} + \frac{2\lambda_{\max}^2(\Lambda_i)}{\lambda_{\min}(\Lambda_i K_i \Lambda_i)} \\ d_{i8} &= \sigma.\end{aligned} \tag{32}$$

It can be easily concluded that the values d_{i1}, d_{i2}, d_{i3}, d_{i5}, d_{i6}, d_{i7}, and d_{i8} are positive. The following condition on ϵ also ensures that d_{i4} is positive:

$$\epsilon < \sqrt[3]{\frac{3\lambda_{\min}(Q)\lambda_{\min}(K_i)\lambda_{\min}(\Lambda_i K_i \Lambda_i)}{16\lambda_{\max}(P)\left(L_{i1}^2\lambda_{\min}(K_i) + L_{i2}^2\lambda_{\min}(\Lambda_i K_i \Lambda_i)\right)}}. \tag{33}$$

From (28) and (31), under the appropriate selection of ϵ according to condition (33), the closed-loop system for the haptic console #i subsystem in combination with the high-gain observer is ISS with respect to state $[\tilde{q}_i^T, \dot{q}_i^T, \tilde{\xi}_i^T, \zeta_i^T]^T$ and the input $[q_{id}^T, \dot{q}_{id}^T, (f_{hi} + f_{ri})^T, \tilde{\xi}_i^*]^T$. □

Up until now, the stability of the haptic devices in a unified formulation in the absence of force reflection term is considered. In the presence of force reflection term, it is no longer possible to proceed with such unified formulation due to the different force reflection term in the two haptic devices. Therefore, the stability of each haptic device is independently studied. Next, the stability of the haptic console #1 subsystem with the force reflection term (15) is investigated.

Proposition 4: The closed-loop system for the haptic console #1 subsystems (1) and (7) with the force reflection term (15) and the high-gain observer (20) is ISS with respect to the state $[\tilde{q}_1^T, \dot{q}_1, \tilde{\xi}_1^T, \zeta_1^T]^T$ and the input $[q_{1d}^T, \dot{q}_{1d}^T, f_e^T, f_{h1}^{*T}, \tilde{\xi}_1^*]^T$.

Proof: The Lyapunov function candidate V_{i2} for $i = 1$ is considered. Then, the derivative of V_{12} is expressed as

$$\begin{aligned}\dot{V}_{12} \leq & -b_{11}\|\tilde{q}_1\|^2 - b_{12}\|\dot{q}_1\|^2 - b_{13}|\tilde{\xi}_1|^2 - b_{14}|\zeta_1|^2 \\ & + b_{15}\|q_{1d}\|^2 + b_{16}\|\dot{q}_{1d}\|^2 + b_{17}(\|f_e\|^2 + \|f_{h1}\|^2) \\ & + b_{18}\left\|\tilde{\xi}_1^*\right\|^2\end{aligned} \tag{34}$$

where $b_{11} = (2/3)\lambda_{\min}(\Lambda_1 K_1 \Lambda_1)$, $b_{12} = (5/8)\lambda_{\min}(K_1)$, and $b_{1j} = d_{1j}$ for $j = 3, 4, ..., 8$. Thus, the closed-loop system is ISS with respect to the state $[\tilde{q}_1^T, \dot{q}_1, \tilde{\xi}_1^T, \zeta_1^T]^T$ and the input $[q_{1d}^T, \dot{q}_{1d}^T, f_e^T, f_{h1}^{*T}, \tilde{\xi}_1^*]^T$ on condition that (33) is satisfied. □

The next step is to study the stability of the haptic console #2 subsystem with the force reflection term (17), as presented in Proposition 5.

Proposition 5: Consider the haptic console #2 subsystems (1) and (7) with the force reflection term (17) and the high-gain observer (20). This system is ISS with respect to the state $[\tilde{q}_2^T, \dot{q}_2, \tilde{\xi}_2^T, \zeta_2^T]^T$ and the input $[q_{2d}^T, \dot{q}_{2d}^T, f_{h2}^{*T}, \tilde{\xi}_2^*]^T$

Proof: The Lyapunov function candidate V_{i2} for $i = 2$ is considered. In the case that $f_{r2} = f_e + f_c$, the inequality $f_{r2} \leq \|f_e\| + \|f_c^s\|$ is obtained where f_c^s is the value of compensating force reflection term when saturated. Next, the value of f_{r2} is substituted in the closed-loop system, and the inequality Assumption 1 is utilized. Then, using Young's inequality, the derivative of V_{22} is expressed as

$$\begin{aligned}\dot{V}_{22} \leq & -b_{21}\|\tilde{q}_2\|^2 - b_{22}\|\dot{q}_2\|^2 - b_{23}|\tilde{\xi}_2|^2 - b_{24}|\zeta_2|^2 \\ & + b_{25}\|q_{2d}\|^2 + b_{26}\|\dot{q}_{2d}\|^2 + b_{27}\left(\|f_c^s\|^2 + \|f_{h2}\|^2\right) \\ & + b_{28}\left\|\tilde{\xi}_2^*\right\|^2\end{aligned} \tag{35}$$

where

$$\begin{aligned}b_{21} &= \frac{1}{2}\lambda_{\min}(\Lambda_2 K_2 \Lambda_2) \\ b_{22} &= \frac{1}{2}\lambda_{\min}(K_2) - \frac{3L_e^2\lambda_{\max}(\Lambda_2 + I)}{\lambda_{\min}(\Lambda_2 K_2 \Lambda_2)} \\ b_{25} &= \frac{4\epsilon^3 L_{i1}^2 \lambda_{\max}(P)}{\lambda_{\min}(Q)} + \frac{2L_e^2}{\lambda_{\min}(K_2)} + \frac{3L_e^2\lambda_{\max}(\Lambda_2)}{\lambda_{\min}(\Lambda_2 K_2 \Lambda_2)}\end{aligned} \tag{36}$$

and $b_{2j} = d_{2j}$ for $j = 3, 4, 6, 7, 8$. To ensure the positivity of b_{25}, the following condition should be satisfied:

$$\frac{\lambda_{\min}(K_2)\lambda_{\min}(\Lambda_2 K_2 \Lambda_2)}{\lambda_{\max}(\Lambda_2 + I)} > 6L_e^2. \tag{37}$$

Thus, the closed-loop system is ISS with respect to the state $[\tilde{q}_2^T, \dot{q}_2^T, \tilde{\xi}_2^T, \zeta_2^T]^T$ and the input $[q_{2d}^T, \dot{q}_{2d}^T, f_e^T, f_{h1}^{*T}, \tilde{\xi}_1^*]^T$ on condition that (33) and (37) are satisfied. □

Finally, the stability analysis of the entire haptic system as our main result of this section is presented in Theorem 1.

Theorem 1: Suppose that the control scheme (7) and the observer (20) are applied to the haptic surgical training system (1). Then, the overall system may be made ISS.

Proof: The ISS small-gain approach of [21] is utilized in the stability analysis of the overall surgery training haptic system. From Proposition 4, the closed-loop system composed of the haptic console #1, the high-gain observer, and the dynamics of human operator is input-to-output (IOS) stable with the input $[q_2^T, \dot{q}_2^T, f_{h1}^{*T}, f_e^T, \xi_1]^T$ and output $[\hat{f}_{h1}^T, q_1^T, \dot{q}_1^T]^T$. Consider that the IOS gain of this system is denoted by γ_1. Furthermore, with a similar reasoning, the closed-loop system is composed of the haptic console #2 is IOS with the input $[q_1^T, \dot{q}_1^T, f_{h2}^{*T}, f_e^T, \xi_2, \hat{f}_{h1}^T]^T$ and output $[q_2^T, \dot{q}_2^T]^T$. It is supposed that γ_2 is the IOS gain of the haptic console #2 subsystem. Note that the gain γ_i for $i = 1, 2$ can be calculated from the ISS stability theorem [18] according to

$$\gamma_i = \frac{a_{i2}a_{i4}}{\kappa a_{i1}a_{i3}} \tag{38}$$

where $0 < \kappa < 1$ and

$$a_{i1} = \min\left(\frac{1}{2}\lambda_{mi}, \lambda_{\min}(\Lambda_i K_i), \frac{1}{2}\gamma_i^{-1}, \lambda_{\min}(P), \lambda_{\min}(K_{hi})\right)$$
$$a_{i2} = \max\left(\frac{1}{2}\lambda_{Mi}, \lambda_{\max}(\Lambda_i K_i), \frac{1}{2}\gamma_i^{-1}, \lambda_{\max}(P), \lambda_{\max}(K_{hi})\right)$$
$$a_{i3} = \max(b_{i1}, b_{i2}, b_{i3}, b_{i4})$$
$$a_{i4} = \max(b_{i5}, b_{i6}, b_{i7}, b_{i8}).$$

From the small-gain theorem, the overall dual-user haptic system is ISS if

$$\gamma_1\gamma_2 < 1 \tag{39}$$

which completes the proof. □

VI. Simulation and Experimental Results

A. Simulation Results

The main purpose of simulation assessments is to investigate the effect of the proposed variable dominance factor and the force reflection term. A fair comparison can be provided by applying similar exogenous inputs force to the system, which can only be done in the simulations and not in the experimental tests. The simulation studies are performed using the dynamical models of two similar Geomagic Touch three degree-of-freedom haptic devices as the haptic consoles [22]. In addition, the contact force of the environment is presumed to be as $f_e(t) = K_e x(t) + B_e \dot{x}(t)$ for $x \geq 0$ and $f_e(t) = 0$ for $x < 0$. The parameters are set to $K_e = 10N/m$, $B_e = 2N.s/m$. Furthermore, the parameters of the operators' hands are set to $M_{hi} = m_{hi}I$, $B_{hi} = b_{hi}I$, and $K_{hi} = k_{hi}I$, where $m_{hi} = 9g$, $b_{hi} = 2N.s/m$, and $k_{hi} = 200N/m$ [7].

As for selecting the control and observer parameters, conditions (37) and (33), as well as the small-gain condition presented in Theorem 1, should be satisfied. First, it is assumed that $K_i = k_i I$, $\Lambda_i = \lambda_i I$, and condition (37) is examined by considering the Lipschitz constant $L_e = 10$. The validity of condition (37) is numerically checked at sufficient sample points in the range of $0 < k_2 < 100$ and $0 < \lambda_2 < 100$. Fig. 4(a) shows the results with the points satisfying (37) in blue stars and the boundary in red line. In order to meet the stability condition (37), it is sufficient to pick up a point from the area shown by blue stars.

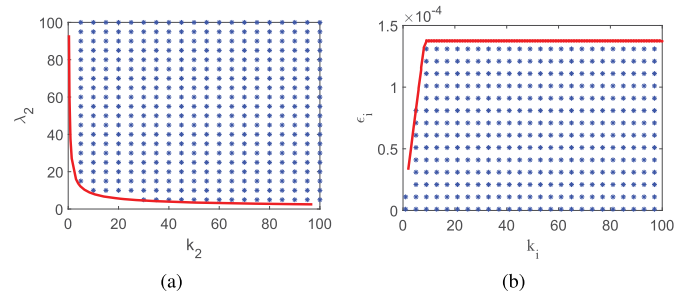

Fig. 4. Regions satisfying stability conditions. (a) Condition (37). (b) Small-gain condition (39).

In order to choose the observer parameters, it is possible to calculate an upper bound for ϵ using (33). The first step for finding such an upper bound is to find the constants L_{i1} and L_{i2} based on the Lipschitz condition (30) using the MATLAB constrained optimization routine. Utilizing the MATLAB function `fmincon` leads to $L_{i1} = L_{i2} = 239.9$. Here, the following bounds are considered for the revolute joints of the robot manipulators in the optimization procedure:

$$-\frac{\pi}{4} \leq q_{i1} \leq \frac{\pi}{4}, \quad 0 \leq q_{i2} \leq \frac{5\pi}{12}, \quad 0 \leq q_{i3} \leq \frac{5\pi}{12} \tag{40}$$

where q_{ij} denotes the jth joint angle of the haptic console #i for $i = 1, 2$, $j = 1, 2, 3$. Next, by considering the observer polynomial parameters $a_1 = 1.4$ and $a_2 = 1$, the Lyapunov equation is solved for P with $Q = 50I$. Then, using (33), the upper bound $\epsilon = 0.02$ is calculated.

Another step is to check the small-gain condition as presented in Theorem 1. Although from (38), the values of γ_i depend on several parameters, our numerical studies have shown that these gains are mostly affected by the control gains K_i and the observer parameters ϵ_i. Thus, other parameters are considered to be fixed and the effect of gains K_i and ϵ_i is studied. The minimum and maximum eigenvalues of the inertia matrix, denoted as λ_m and λ_M, respectively, are computed using the MATLAB function `fmincon` by considering the joint limits (40). It is also considered that $\lambda_i = 10$ and the adaptation gains are set to $\gamma_i = 0.1$, $\sigma_i = 0.1$ for $i = 1, 2$, and the parameter θ introduced in Theorem 1 is selected as $\theta = 0.9$. The small-gain condition (39) is then numerically examined at a number of sample points in the range of $0 < k_i < 100$ and $0 < \epsilon_i < 0.001$ for $i = 1, 2$ with the assumption that $k_1 = k_2$ and $\epsilon_1 = \epsilon_2$. Fig. 4(b) shows the results with the points in which the small-gain condition is met in blue stars and the boundary in red line. In order to satisfy the small-gain condition, it is sufficient to pick up a point from the area shown by blue stars. In this research, these parameters are selected as $k_1 = k_2 = 10$ and $\epsilon_1 = \epsilon_2 = 10^{-4}$.

Furthermore, the parameters related to the proposed methodology for online authority adjustment and compensating force reflection term are selected as $w = 2$ s, $\beta_1 = 0.25$, $\beta_2 = 0.26$, $\rho_1 = 1.5$, and $\rho_2 = 2$. To study the robustness of the

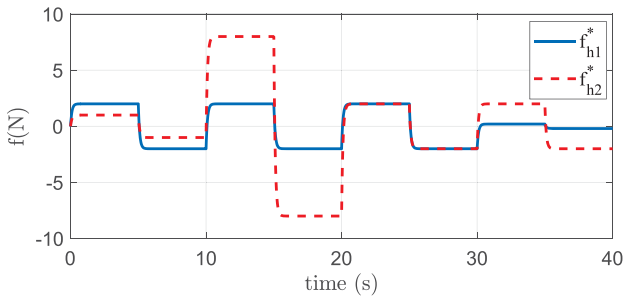

Fig. 5. Simulation: exogenous forces applied by users.

proposed structure, all of the physical parameters are randomly perturbed by up to 20% in the controller and the observer with respect to their nominal values.

Fig. 5 shows the trainer's and the trainee's exogenous forces applied in the x-direction for the simulations. These forces constitute a train of pulse passed through the filter $(1/0.1s + 1)$. The correct force signal is presumed to have the steady-state value of $2N$. Thus, from $t = 0$ s to $t = 10$ s and from $t = 10$ s to $t = 20$ s, the trainee does not exert the correct force command and the task is controlled by the trainer. The amplitude of the force applied by the trainee from $t = 0$ s to $t = 10$ s is less than the correct force but is extremely higher than the correct force from $t = 10$ s to $t = 20$ s. Besides, from $t = 20$ s to $t = 30$ s, the trainee applies correct force but the task authority is still maintained by the trainer. Finally, from $t = 30$ s to $t = 40$ s, the trainee applies correct force, and the task authority is transformed to the trainee.

In order to investigate various aspects of the proposed control approach, the simulations are performed in three cases: case 1) the proposed adaptive robust control architecture with fixed dominance factor, i.e., $\alpha = 0$, and without considering the compensating force reflection term; case 2) the proposed adaptive robust control architecture with the variable dominance factor obtained from (5) with no force reflection term; and case 3) the proposed adaptive robust control architecture with variable dominance factor and the compensating force reflection term.

The positions of the haptic consoles as well as the dominance factor for all three cases are shown in Fig. 6. In case 1) where $\alpha = 0$, we expect that the task be fully controlled by the trainee, and the trainer is not able to interfere with the procedure to correct the trainee's movements even if the trainee performs wrong movements. Therefore, in the first case, the task is fully controlled by the trainee and the trainer only receives the trainee's position command through the haptic channel. The results of case 1) in Fig. 6(a) verify this expectation as the positions are in full accordance with the magnitude of the exogenous force applied by the trainee.

For case 2), it is expected that the task authority is transformed to the trainer according to (5), provided that the moving average of the force exerted by the trainer is greater than the predefined value ρ_2. Otherwise, the task is fully controlled by the trainee. Therefore, it is expected from the exogenous force pattern that the task is controlled by the trainer during $t = 0$ s to $t = 30$ s, while it is controlled by the trainee from $t = 30$ s to $t = 40$ s. The positions

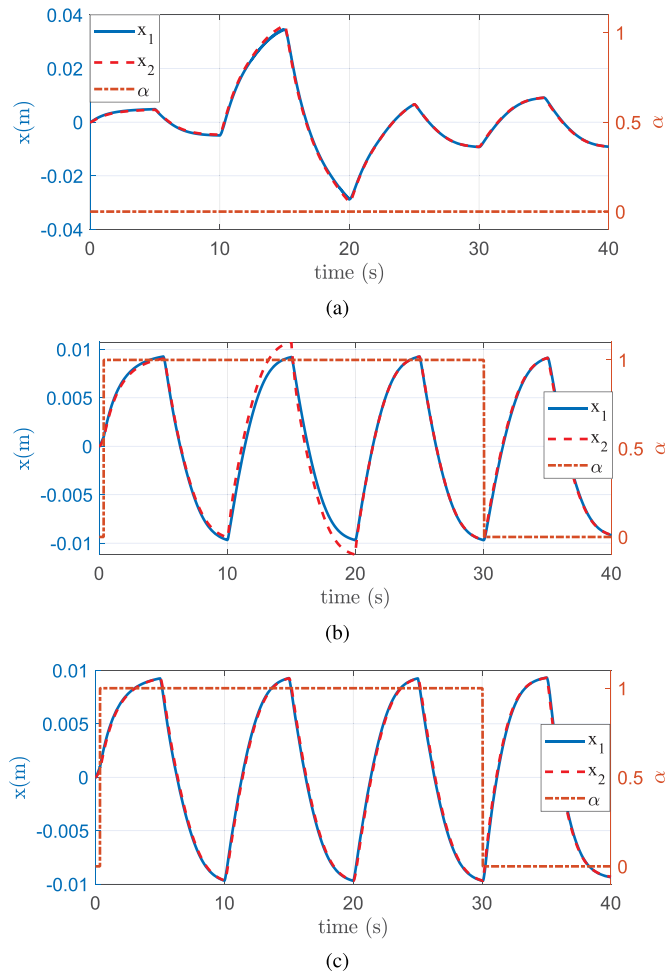

Fig. 6. Simulation: The position of the trainer's and trainee's hands and the dominance factor. (a) First case. (b) Second case. (c) Third case.

as shown in Fig. 6(b) verify such expectation as the position signals from $t = 0$ s to $t = 10$ s, $t = 10$ s to $t = 20$ s, and $t = 20$ s to $t = 30$ s mostly follow the trainer's input pattern and from $t = 30$ s to $t = 40$ s follow the trainee's command. However, the position tracking from $t = 10$ s to $t = 20$ s is not satisfactory due to the high amount of exogenous force applied by the trainee. Obviously, the force applied by the trainee is in the retaining region from $t = 0$ s to $t = 10$ s and from $t = 20$ s to $t = 30$ s and does not have any considerable adverse effect in these periods of time. However, the distance between the forces applied by the trainee and the trainer exceeds the upper threshold ρ_2 and the controller enters to the compensating region. Since the compensating force reflection term is not included in case 2), the large magnitude of the trainee's force significantly affects the position tracking.

On the other hand, in case 3), the controller enters the compensating region for the period $t = 20$ s to $t = 30$ s, and the adverse effect of the trainee's large exogenous force is compensated, resulting in satisfactory position tracking, as shown in Fig. 6(c) for $t = 20$ s to $t = 30$ s.

To investigate the performance of the proposed high-gain observer, the real and estimated force signals of the trainer's hand and the trainee's hand are shown in Fig. 7(a) and (b),

This article has been accepted for inclusion in a future issue of this journal. Content is final as presented, with the exception of pagination.

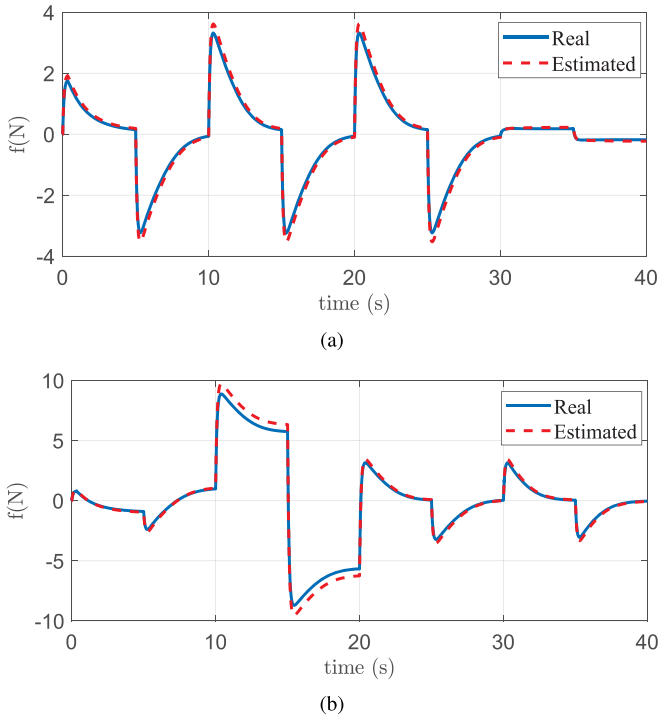

Fig. 7. Simulation: The real and estimated force signals. (a) Trainer's hand force. (b) Trainee's hand force.

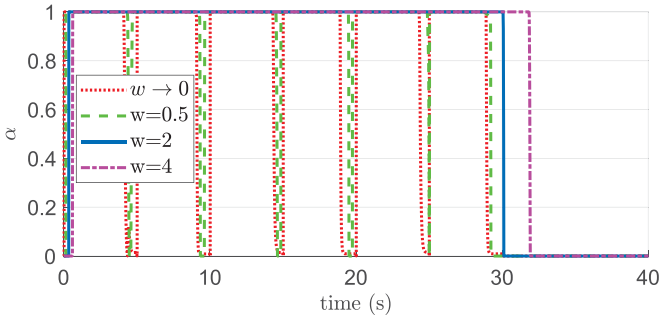

Fig. 8. Simulation: Effect of window size.

respectively. It is apparent that the high-gain observer provides an accurate estimate of the hand force.

It should be noted that the selection of window size in averaging the trainer's hand force for the adjustment of the dominance factor is an important factor in the proposed approach since small values lead to short-term fluctuations, while large values induce lag in the control system. Fig. 8 illustrates the dominance factor for various window sizes $w = 0, 0.5, 2$, and 4 s. The (red) dotted line shows dominance factor for zero window size, implying that the instantaneous values of the hand force determine the dominance factor. Such a choice leads to several short-term fluctuations, which are expected to have a detrimental effect on the system performance. Similar trend, in dashed (green) line, is also observed for $w = 0.5$. The solid (blue) line demonstrates the dominance factor for $w = 2$, which is the value selected for the simulations that had already been presented. This selection seems to be suitable since it rather put emphasis on longer term trends and better represent the intention of the trainer. Finally, the

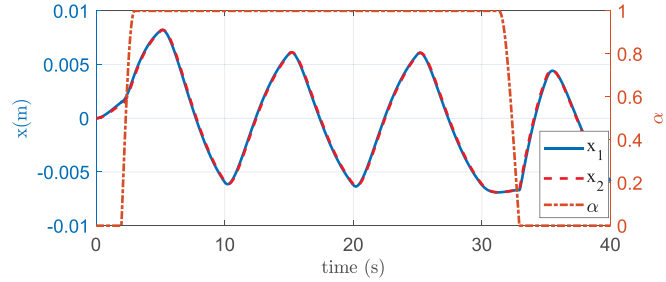

Fig. 9. Simulation: The position signals and the dominance factor.

case with the larger window size, i.e., $w = 4$, is shown by dashed-dotted (magenta) line. In this case, the larger window size introduces an undue delay in the transfer of task authority.

Furthermore, adjustment of the transition state is another important feature of the proposed architecture. As already explained, the transition state is considered to avoid abrupt switching in the controller and for the smooth behavior of the system. However, the duration of the transition is intentionally set as small as possible to ensure prompt action of the controller. Here, we present another simulation to study the effect of slower transition state on the performance of the system. For that purpose, the exogenous forces applied to the system are obtained by the same train of pulses as that of the previous simulations, but the force signals of the new simulation are passed through the filter with $(1/2.5\ \text{s} + 1)$. Besides, the window size of the moving average is set as $w = 4$, and the width of transition in (5) is set as $\Delta\beta = 0.2$. The parameters β_1 is selected the same as that of the previous experiment. The other parameters are also set as that of case 3) in the previous simulation. Such a selection of the parameters leads to slower transition state. The simulation results are depicted in Fig. 9. Although the results show the stable behavior of the signals with a gradual change of dominance factor between 0 and 1, the slow switch of task authority prevents immediate action of the control scheme. As an illustration, the trainer tries to transform the task authority at the beginning of the simulation and at $t \approx 30$. However, the gradual change of dominance factor introduces an undue delay in the transfer of task authority and prevents fast action of the controller. This situation is more critical when the trainer tries to interfere with the procedure to correct the trainee's movement. In that case, the delay in the transfer of task authority impedes quick intervention of the trainer. As such, the parameters related to the transition state in the real experiment should be selected sufficiently small. However, too small transition state may cause jumps in the control action owing to the effect of hard switching. Therefore, the duration of the transition is designed based on a tradeoff between the swift action of the controller and the smoothness of the signals.

B. Experimental Results

The experimental setup employed for the evaluation of the proposed control methodology is depicted in Fig. 10. The setup consists of two 3-DOF Geomagic Touch haptic devices (consoles). Data are exchanged between the haptic consoles through the user datagram protocol (UDP)-based communication channel. OpenHaptics software development kit (SDK)

This article has been accepted for inclusion in a future issue of this journal. Content is final as presented, with the exception of pagination.

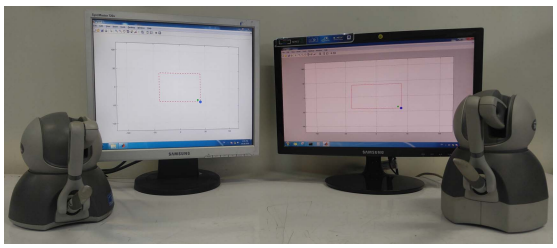

Fig. 10. Dual-user experimental setup.

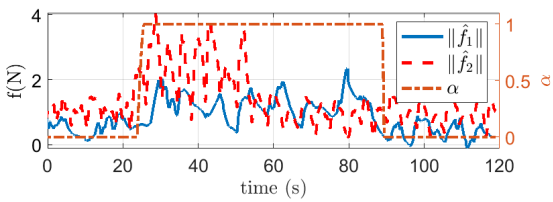

Fig. 11. Norm of the estimated forces and the dominance factor.

is utilized to implement the proposed controller. The control loop runs at the rate of 1 kHz. Notably, the haptic console and workspace considered in the simulation section are the same as the one utilized in the experiments with the same parameters. Therefore, the stability conditions derived in the simulation section are valid for the experiments. As already explained, the duration of transition should be set based on a tradeoff between the swift action of the controller and the smoothness of the signals. In the experiments, the parameters related to the transition state are selected as $w = 2$ s, $\beta_1 = 0.55$, and $\beta_2 = 0.65$.

The task under study is to follow a 2-D square path. Each user observes her/his own hand position with respect to the square path in the xy plane on a display as well as the other user' hand position. The haptic console #1 and haptic console #2 are interfaced with the trainer and the trainee, respectively.

The norm of the estimated hand force of the operators and the dominance factor is depicted in Fig. 11. The estimated hand force of the trainer is depicted by solid (blue) line, whereas the estimated hand force of the trainee is shown by dashed (red) line. The right vertical axis shows the dominance factor. It is apparent that the trainer exerts low magnitude of force from $t = 0$ s to $t \approx 22$ s and from $t \approx 85$ s to $t = 120$ s; hence, the task authority is transformed to the trainee in those periods of time. By exerting considerable amount of force from $t \approx 22$ s to $t \approx 80$ s, the trainer holds the task authority. In the time between $t \approx 22$ s and $t \approx 55$ s, the trainee is asked to deliberately exert extra force signals in order to study the behavior of the system in the compensating region.

Moreover, the xy positions and the positions of the first joint for both the trainer and the trainee are depicted in Figs. 12 and 13, respectively, and the position error for the first joint is shown in Fig. 14. In Figs. 12 and 13, the position of the trainer is depicted by solid (blue) line, whereas the position of the trainee is shown by dashed (red) line. At the first step of training from $t = 0$ s to $t \approx 22$ s, the trainer grants task authority to the trainee to evaluate his skill in drawing a square by applying a low amount of force.

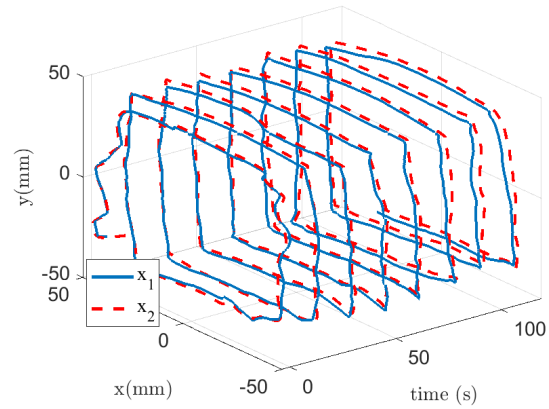

Fig. 12. xy positions of haptic consoles.

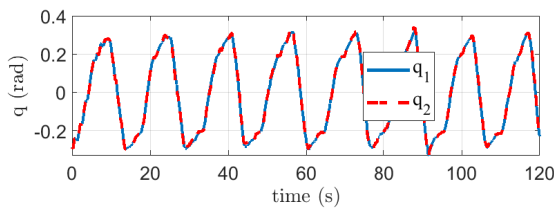

Fig. 13. Positions of the first joint.

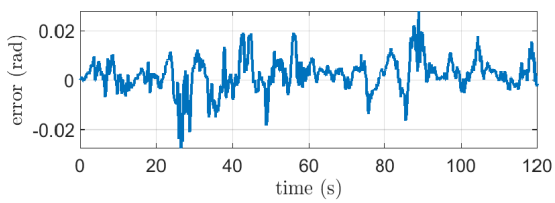

Fig. 14. Position errors of the first joint.

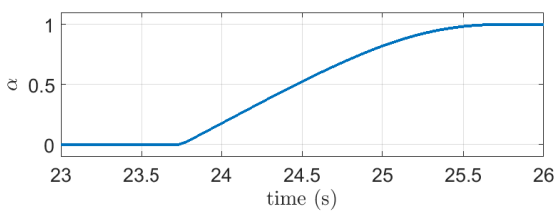

Fig. 15. Transition of dominance factor (zoomed plot).

At this time, the trainee is supposed to not have sufficient experience in performing the task; thus, the task is not performed well. This issue is apparent in the position signal in xy depicted in Fig. 12. Then, at $t \approx 22$ s, the task authority is transferred back to the trainer so the trainee can acquire skills for performing the task. Despite larger forces exerted by the trainee from $t \approx 22$ s to $t \approx 55$ s, the position signals show acceptable tracking performance in that period of time. From $t \approx 55$ s to $t \approx 85$ s, the task authority still remains with the trainer; while the trainee is provided a chance to learn the task. Finally, from $t \approx 85$ s to $t = 120$ s, the task authority is transferred back to the trainee. The position signals show that the trainee's performance in drawing square is acceptable in this time period as can be seen in the xy plot as shown

in Fig. 12. Besides, the tracking performance of the proposed control approach in both trainee-dominant mode and trainer-dominant mode is satisfactory. Finally, the zoomed plot of dominance factor depicted in Fig. 15 demonstrates a smooth transition state for the dominance factor.

VII. Conclusion

In this article, an adaptive robust control methodology with online authority adjustment is presented for a surgical training haptic system. Two primary operation modes, namely, trainee-dominant and trainer-dominant modes are realized to provide the trainer with the opportunity to transfer the task authority to and from the trainee in real time. The stability of the closed-loop system is rigorously analyzed using the ISS stability theory. Simulation and experimental results demonstrate the effectiveness of the proposed approach. Future work includes user studies to evaluate task performance in comparison with benchmark controllers.

Appendix

A. Proof of Proposition 1

The following Lyapunov function candidate is considered:

$$V_{i1} = \frac{1}{2} r_i^T M_i(q_i) r_i + \tilde{q}_i^T \Lambda_i K_i \tilde{q}_i + \frac{1}{2}\gamma_i^{-1}\tilde{\xi}_i^2. \tag{41}$$

Calculating $\dot{V}_{i1}$ and using Property 2 yields

$$\begin{aligned}\dot{V}_{i1} = &-r_i^T K_i r_i + 2\tilde{q}_i^T \Lambda_i K_i \dot{q}_i - 2\tilde{q}_i^T \Lambda_i K_i \dot{q}_{id} \\ &+ r_i^T Y_i(\hat{\theta}_i - \theta_i) + r_i^T f_{hi} + \gamma^{-1}\dot{\tilde{\xi}}_i \tilde{\xi}_i.\end{aligned} \tag{42}$$

On the other hand, from (11) and (12), it can be verified that

$$\begin{aligned} r_i^T Y_i(\hat{\theta}_i - \theta_i) &= r_i^T Y_i\left(\theta_i^* - \theta_i + \delta\theta_i\right) \\ &\le \xi_i \left\| Y_i^T r_i \right\|_1 - \hat{\xi}_i r_i^T Y_i \mathrm{sat}\left(Y_i^T r_i\right) \\ &= \tilde{\xi}_i \left\| Y_i^T r_i \right\|_1. \end{aligned} \tag{43}$$

Hence, using (43) and (14), the following inequality is obtained:

$$\begin{aligned}\dot{V}_{i1} \le &-\dot{q}_i^T K_i \dot{q}_i - \tilde{q}_i^T \Lambda_i K_i \Lambda_i \tilde{q}_i - \sigma \tilde{\xi}_i^2 \\ &-2\tilde{q}_i^T \Lambda_i K_i \dot{q}_{id} + r_i^T f_{hi} + \sigma \tilde{\xi}_i \tilde{\xi}_i^*.\end{aligned} \tag{44}$$

Next, from the well-known Young's quadratic inequality [20], it can be concluded that

$$\begin{aligned}\dot{V}_{i1} \le &-c_{i1}\|\tilde{q}_i\|^2 - c_{i2}\|\dot{q}_i\|^2 - c_{i3}|\tilde{\xi}_i|^2 \\ &+ c_{i4}\|\dot{q}_{id}\|^2 + c_{i5}\|f_{hi}\|^2 + c_{i6}\|\tilde{\xi}_i^*\|^2\end{aligned} \tag{45}$$

where

$$\begin{aligned} c_{i1} &= \frac{5}{6}\lambda_{\min}(\Lambda_i K_i \Lambda_i) \\ c_{i2} &= \frac{7}{8}\lambda_{\min}(K_i) \\ c_{i3} &= \frac{3}{4}\sigma \\ c_{i4} &= \frac{12\lambda_{\max}(\Lambda_i K_i)}{\lambda_{\min}(\Lambda_i K_i \Lambda_i)} \\ c_{i5} &= \frac{2}{\lambda_{\min}(K_i)} + \frac{3\lambda_{\max}^2(\Lambda_i)}{\lambda_{\min}(\Lambda_i K_i \Lambda_i)} \\ c_{i6} &= \sigma. \end{aligned}$$

From (41) and (45), the closed-loop system for the haptic console #1 subsystem is ISS with respect to the state $[r_i^T, \tilde{q}_i^T, \tilde{\xi}_i^T]^T$ and the input $[\dot{q}_{id}^T, f_{hi}^T, \tilde{\xi}_i^*]^T$. Therefore, it is ISS with respect to the state $[\tilde{q}_i^T, \dot{q}_i, \tilde{\xi}_i^T]^T$ and the input $[\dot{q}_{id}^T, f_{hi}^T, \tilde{\xi}_i^*]^T$. □

B. Proof of Proposition 2

First, on account of the fact that the function V_i is an ISS Lyapunov function for the system (1) there exists class $\mathcal{K}_\infty$ functions α_1 and α_2, a class $\mathcal{K}$ function ρ, and a positive definite function W, such that

$$\alpha_1(\|\chi\|) \le V_i \le \alpha_2(\|\chi\|) \tag{46}$$

$$\dot{V}_i \le -W(\|\chi\|) \qquad \forall \|\chi\| \ge \rho(\|\mu\|) \tag{47}$$

where $\dot{V}_i$ is the derivative of V_i along the trajectories of (1). Next, by computing the derivative of the Lyapunov function V_i from (26) and substituting the term $M_i(q_i)\ddot{q}_i$ from (1) and using property 2, the following inequality is obtained:

$$\dot{V}_i = -\dot{q}_i^T g_i(q_i) + \dot{q}_i^T u_i + \dot{q}_i^T J^T f_h + \dot{V}_{ic}. \tag{48}$$

Therefore, using (47) and (48), the following inequality is obtained:

$$\begin{aligned}-\dot{q}_i^T g_i(q_i) + \dot{q}_i^T u_i + \dot{q}_i^T J_i^T(q_i) f_{hi} + \dot{V}_{ic} \le -W(\|\chi\|) \\ \forall \|\chi\| \ge \rho(\|\mu\|).\end{aligned} \tag{49}$$

On the other hand, by substituting (3) into (1), the following dynamics is achieved:

$$\mathcal{M}_i(q_i)\ddot{q}_i + \mathcal{C}_i(q_i, \dot{q}_i)\dot{q}_i + \mathcal{G}_i(q_i) = u_i + J_i^T(q_i) f_{hi}^* \tag{50}$$

where

$$\begin{aligned} \mathcal{M}_i(q_i) &= M_i(q_i) + J_i^T(q_i) M_{hi} J_i(q_i) \\ \mathcal{C}_i(q_i, \dot{q}_i) &= C_i(q_i, \dot{q}_i) + J_i^T(q_i) M_{hi} \dot{J}_i(q_1) + J_i^T(q_i) B_{hi} J_i(q_i) \\ \mathcal{G}_i(q_i) &= G_i(q_i) + J_i^T(q_i) K_{hi} x_i. \end{aligned}$$

Now, consider the following Lyapunov Candidate function:

$$V_{it} := V_i + \frac{1}{2}\dot{x}_i M_{hi} \dot{x}_i + \frac{1}{2} x_i^T K_{hi} x_i.$$

From (46) and the positive definiteness of M_{hi} and K_{hi}, there exist class $\mathcal{K}$ functions $\alpha_5(.)$ and $\alpha_6(.)$ such that

$$\alpha_5(\|\chi_a\|) \le V_{it} \le \alpha_6(\|\chi_a\|) \tag{51}$$

where χ_a is the state vector of the new system. On the other hand, using (26)–(27), it is possible to show that V_{it} in (B) is equivalent to

$$V_{it} = V_{ic} + \frac{1}{2}\dot{q}_i \mathcal{M}_i(q_i)\dot{q}_i + \frac{1}{2} x_i^T K_{hi} x_i. \tag{52}$$

Next, by calculating the derivative of the function V_{i2} from (52) and substituting the term $\mathcal{M}_i(q_i)\ddot{q}_i$ from (50), the following relation is obtained:

$$\begin{aligned}\dot{V}_{it} = &-\dot{q}_i^T J_i^T(q_i) B_{hi} J_i(q_i)\dot{q}_i - \dot{q}_i^T g_i(q_i) + \dot{q}_i^T u_i + \dot{q}_i^T J^T f_h^* \\ &+ \dot{V}_{ic}.\end{aligned}$$

Now, from (49), it can be concluded that

$$\dot{V}_i \leq -W(\|\chi\|) \qquad \forall \|\chi\| \geq \rho(\|\mu_a\|) \tag{53}$$

where $\alpha_7(.)$ and $\alpha_8(.)$ are class $\mathcal{K}$ functions and $\mu^a = [\eta^T, f_{hi}^{*T}]^T$. The statements (51) and (53) show that the system is ISS with input $\mu_a = [\eta^T, f_{hi}^{*T}]^T$ and state χ, which completes the proof. □

REFERENCES

[1] B. Hannaford and A. M. Okamura, "Haptics," in *Springer Handbook of Robotics*. Berlin, Germany: Springer, 2016, pp. 1063–1084.

[2] Z. Kowalczuk and M. Tatara, "Sphere drive and control system for haptic interaction with physical, virtual, and augmented reality," *IEEE Trans. Control Syst. Technol.*, vol. 27, no. 2, pp. 588–602, Mar. 2019.

[3] M. Motaharifar, H. D. Taghirad, K. Hashtrudi-Zaad, and S.-F. Mohammadi, "Control synthesis and ISS stability analysis of a dual-user haptic training system based on S-shaped function," *IEEE/ASME Trans. Mechatronics*, vol. 24, no. 4, pp. 1553–1564, Aug. 2019.

[4] S. F. Atashzar, M. Shahbazi, M. Tavakoli, and R. V. Patel, "A passivity-based approach for stable patient–robot interaction in haptics-enabled rehabilitation systems: Modulated time-domain passivity control," *IEEE Trans. Control Syst. Technol.*, vol. 25, no. 3, pp. 991–1006, May 2017.

[5] I. Sharifi, H. A. Talebi, and M. Motaharifar, "A framework for simultaneous training and therapy in multilateral tele-rehabilitation," *Comput. Elect. Eng.*, vol. 56, pp. 700–714, Nov. 2016.

[6] S. S. Nudehi, R. Mukherjee, and M. Ghodoussi, "A shared-control approach to haptic interface design for minimally invasive telesurgical training," *IEEE Trans. Control Syst. Technol.*, vol. 13, no. 4, pp. 588–592, Jul. 2005.

[7] B. Khademian and K. Hashtrudi-Zaad, "Dual-user teleoperation systems: New multilateral shared control architecture and kinesthetic performance measures," *IEEE/ASME Trans. Mechatronics*, vol. 17, no. 5, pp. 895–906, Oct. 2012.

[8] F. Hashemzadeh, M. Sharifi, and M. Tavakoli, "Nonlinear trilateral teleoperation stability analysis subjected to time-varying delays," *Control Eng. Pract.*, vol. 56, pp. 123–135, 2016.

[9] M. Shahbazi, S. F. Atashzar, H. A. Talebi, and R. V. Patel, "An expertise-oriented training framework for robotics-assisted surgery," in *Proc. IEEE Int. Conf. Rob. Autom.*, May/Jun. 2014, pp. 5902–5907.

[10] Z. Lu, P. Huang, P. Dai, Z. Liu, and Z. Meng, "Enhanced transparency dual-user shared control teleoperation architecture with multiple adaptive dominance factors," *Int. J. Control, Autom. Syst.*, vol. 15, no. 5, pp. 2301–2312, Oct. 2017.

[11] H. Wang, C. C. Cheah, W. Ren, and Y. Xie, "Passive separation approach to adaptive visual tracking for robotic systems," *IEEE Trans. Control Syst. Technol.*, vol. 26, no. 6, pp. 2232–2241, Nov. 2018.

[12] M. Motaharifar, H. A. Talebi, F. Abdollahi, and A. Afshar, "Nonlinear adaptive output-feedback controller design for guidance of flexible needles," *IEEE/ASME Trans. Mechatronics*, vol. 20, no. 4, pp. 1912–1919, Aug. 2015.

[13] H. K. Khalil, "Extended high-gain observers as disturbance estimators," *SICE J. Control Meas. Syst. Integr.*, vol. 10, no. 3, pp. 125–134, 2017.

[14] M. W. Spong and M. Vidyasagar, *Robot Dynamics and Control*. Hoboken, NJ, USA: Wiley, 2008.

[15] M. Vukobratovic, D. Surdilovic, Y. Ekalo, and D. Katic, *Dynamics and Robust Control of Robot-Environment Interaction*. Singapore: World Scientific, 2009.

[16] K. Razi and K. Hashtrudi-Zaad, "Analysis of coupled stability in multilateral dual-user teleoperation systems," *IEEE Trans. Robot.*, vol. 30, no. 3, pp. 631–641, Jun. 2014.

[17] A. Takhmar, I. G. Polushin, A. Talasaz, and R. V. Patel, "Cooperative teleoperation with projection-based force reflection for MIS," *IEEE Trans. Control Syst. Technol.*, vol. 23, no. 4, pp. 1411–1426, Jul. 2015.

[18] H. K. Khalil, *Nonlinear Systems*. Upper Saddle River, NJ, USA: Prentice-Hall, 2002.

[19] H. J. Márquez, *Nonlinear Control Systems: Analysis and Design*. Hoboken, NJ, USA: Wiley, 2003.

[20] H. L. Royden and P. Fitzpatrick, *Real Analysis*, 4th ed. Boston, MA, USA: Prentice-Hall, 2010.

[21] I. G. Polushin, A. Tayebi, and H. J. Marquez, "Control schemes for stable teleoperation with communication delay based on IOS small gain theorem," *Automatica*, vol. 42, no. 6, pp. 905–915, Jun. 2006.

[22] E. Naerum, J. Cornella, and O. J. Elle, "Contact force estimation for backdrivable robotic manipulators with coupled friction," in *Proc. IEEE/RSJ Int. Conf. Intell. Robots Syst.*, Sep. 2008, pp. 3021–3027.

Mohammad Motaharifar (S'10) received the B.Sc. degree in electrical engineering from the Iran University of Science and Technology, Tehran, Iran, in 2009, the M.Sc. degree in electrical engineering from the Amirkabir University of Technology, Tehran, in 2011, and the Ph.D. degree in electrical engineering from the K. N. Toosi University of Technology, Tehran, in 2019.

He was a Visiting Research Assistant with the Department of Electrical and Computer Engineering, Queen's University, Kingston, ON, Canada, in Fall 2018 Semester. His current research interests include medical robotics, nonlinear control, and robust control.

Hamid D. Taghirad (SM'12) received the B.Sc. degree in mechanical engineering from the Sharif University of Technology, Tehran, Iran, in 1989, and the M.Sc. degree in mechanical engineering and the Ph.D. degree in electrical engineering from McGill University, Montreal, QC, Canada, in 1993 and 1997, respectively.

He is currently a Professor and the Vice Chancellor for Global Strategies and International Affairs and the Director of the Advanced Robotics and Automated System, K.N. Toosi University of Technology, Tehran. He has authored or coauthored five books and more than 190 articles in international journals and conference proceedings. His current research interest includes robust and nonlinear control applied to robotic systems.

Dr. Taghirad is a member of the board of the Industrial Control Center of Excellence, K. N. Toosi University of Technology. He is the Editor-in-Chief of *Mechatronics Magazine* and a member of the Editorial Board of the *International Journal of Robotics: Theory and Application* and the *International Journal of Advanced Robotic Systems*.

Keyvan Hashtrudi-Zaad (SM'08) received the Ph.D. degree in electrical and computer engineering from the University of British Columbia, Vancouver, BC, Canada, in 2000.

He then held a consulting position with Motion Metrics International Corporation, Vancouver, where he was involved in the development of a dynamic payload monitoring system for heavy duty hydraulic machines. In 2001, he joined the Department of Electrical and Computer Engineering, Queens University, Kingston, ON, Canada, where he is currently a Professor and the Co-Director of the BioRobotics Research Laboratory. His current research interests include telerobotics, haptics, telerehabilitation, autonomous driving, and control systems.

Dr. Hashtrudi-Zaad served as an Associate Editor for the IEEE TRANSACTIONS ON HAPTICS and on the organization committees of a number of IEEE-sponsored conferences.

Seyed Farzad Mohammadi received the Fellowship degree in anterior segment of the eye from the Tehran University of Medical Sciences, Tehran, Iran, in 2007.

He is currently an Associate Professor of ophthalmology with Translational Ophthalmology Research Center, Farabi Eye Hospital, Tehran University of Medical Sciences. His current research interests include bench-to-bedside researches and ophthalmic epidemiology.

Mr. Mohammadi is board-certified in ophthalmology and a fellow of the International Council of Ophthalmology.